

Gyromagnetic damping and the role of spin-wave generation in pulsed inductive microwave magnetometry

M. L. Schneider, Th. Gerrits, A. B. Kos, and T. J. Silva

National Institute of Standards and Technology, Electromagnetics Division, Boulder, Colorado 80305

(Received 14 March 2005; accepted 30 June 2005; published online 12 August 2005)

The dependence of the magnetodynamic response of thin permalloy films was measured with a pulsed inductive microwave magnetometer as a function of varying width of the coplanar waveguide center conductor (220 to 990 μm), frequency (0.6 to 2 GHz) and film thickness (25 to 93 nm) to ascertain the role of magnetostatic spin-wave generation in the low-frequency enhancement of the measured decay rate. A component of the decay rate depends on δ_w , the ratio of film thickness to center conductor width as theoretically predicted. However, there is an anomalous contribution to the frequency dependence of the decay rate exists that cannot be attributed to the generation of spin-waves. [DOI: 10.1063/1.2031944]

To improve the performance of magnetoelectronic devices, a better understanding of the detailed magnetodynamics is desired. In particular, there is a need to understand damping in practical magnetic alloys such as $\text{Ni}_{81}\text{Fe}_{19}$ (permalloy). An increasingly popular technique for measuring magnetodynamic properties is the pulsed inductive microwave magnetometer (PIMM).

A PIMM uses a coplanar waveguide (CPW) structure as both the excitation source and the inductive detector of damped ferromagnetic precession. Free induction decay experiments using both pulsed^{1–3} and continuous wave^{4–6} excitation have been demonstrated using a coplanar waveguide geometry. Recent studies have shown a shift in the resonance frequency⁷ and a change in the decay rate associated with the width of the center conductor of the CPW line.^{5,7} However, an experimental study in which both the film thickness and the CPW center conductor width are varied systematically to observe their influence on the decay rate has not yet been performed.

In this study, we report the results of such experiments for three center conductor widths of 220, 525, and 990 μm , and four film thicknesses of 25, 46, 68, and 93 nm. We find a qualitative dependence of the decay rate on the ratio of film thickness to center conductor width that is consistent with the generation of a continuous band of magnetostatic modes. However, the dependence does not completely explain the larger than expected increase in decay rate at low frequencies.

The films used in this study were polycrystalline permalloy films grown by dc magnetron sputtering in a 0.533 Pa Ar atmosphere and an applied field to induce a uniaxial anisotropy and have been described in detail in Ref. 7. The film thicknesses were determined using a profilometer after deposition. The magnetic properties of the films were characterized with a quasi-static inductive magnetometer. The easy-axis coercivity was 178 ± 23 A/m and the uniaxial anisotropy was 377 ± 24 A/m.

Each CPW used in the PIMM had a characteristic impedance of $50 \pm 1 \Omega$. The easy-axis of the films was aligned parallel to the center conductor. To minimize any change in impedance due to the presence of the thin films, the bare side of the substrate was placed on top of the CPW such that the film side was away from the CPW. A floating ground plane

was positioned above the sample to enhance the magnetic field pulse.⁸ We estimate that the magnetic field pulse was 366 A/m. In addition, we confirmed that there is no change in the results derived from our measurements when the pulse field is reduced from 80 A/m, consistent with previously obtained PIMM measurements.⁸ A detailed description of the PIMM and the data acquisition process can be found in Refs. 1–3.

It has been proposed that one should fit decay rate data obtained using a CPW structure with standard Landau–Lifshitz–Gilbert (LLG) damping plus a contribution due to the generation of broad-band spin-waves.⁵ Spin-wave generation arises because the film is excited by a spatially inhomogeneous field pulse. The in-plane wave vector, k_{\parallel} , of the excited spin-waves is determined by the non-uniform excitation. As such, the maximum k_{\parallel} is set by the width w of the CPW center conductor. The shortest wavelength that can be efficiently driven by the CPW is $\lambda \approx 2w$, corresponding to $k_{\text{max}} \approx \pi/w$ in reciprocal space. We are operating in the thin film limit of $k_{\parallel}\delta \ll 1$, where δ is the film thickness. In addition, the width of our CPW center conductor is much greater than the exchange length of 6 nm. Thus, we are exciting magnetostatic waves with a uniform magnetization distribution through the film thickness. Using the conventional model for spin-wave generation by a CPW antenna structure proposed by Council *et al.*,⁵ we can estimate the spin-wave contribution to the ferromagnetic resonance width using the equation

$$\Delta\omega(k_{\text{max}}) = \Delta\omega_{\text{int}} \sqrt{1 + \left(\frac{\omega_s(k_{\text{max}}) - \omega_0}{\Delta\omega_{\text{int}}} \right)^2}, \quad (1)$$

where $\Delta\omega(k_{\text{max}})$ is the total line-width for a distribution of spin-waves of uniform amplitude, with $0 < k_{\parallel} < k_{\text{max}}$, $\Delta\omega_{\text{int}}$ is the intrinsic Landau–Lifshitz frequency-swept line-width for the material in question, and ω_0 is the center resonance frequency. The spin-wave frequency is given by Ref. 5 as $\omega_s(k_{\text{max}}) = \sqrt{\omega_0^2 + \frac{1}{2}\omega_M^2 k_{\text{max}} \delta}$, where $\omega_M = \gamma\mu_0 M_s$, and $|\gamma| = (g\mu_B)/\hbar$ is the gyromagnetic ratio, g is the spectroscopic splitting factor, μ_B is the Bohr magneton, $\mu_0 = 4\pi \times 10^{-7}(\text{H/m})$ is the permeability of free space, M_s is the saturation magnetization which for our films was assumed to be ~ 830 kA/m. The intrinsic line-width $\Delta\omega_{\text{int}}$ is related to

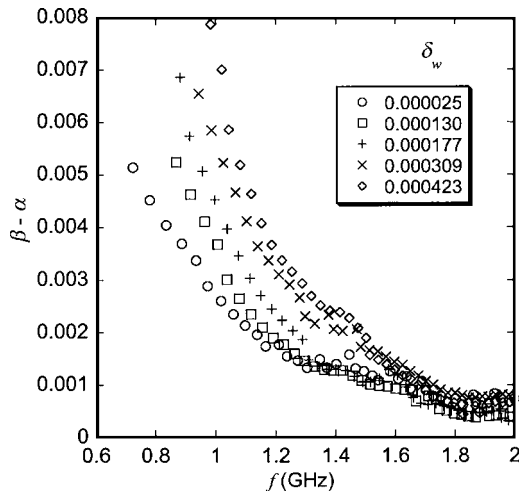


FIG. 1. The normalized decay rate, β , data with the LLG damping component, α , subtracted for five different combinations of sample thickness and waveguide width clearly exhibit an increase in decay rate at low frequencies. As δ_w is increased, the effect becomes more pronounced.

the Landau–Lifshitz damping parameter α through $\Delta\omega_{\text{int}} \approx \alpha\omega_M$. Equation (1) presumes that the wave-vector is perpendicular to the average magnetization direction. This approximation is valid for our experimental geometry in the limit of small pulse fields. Equation (1) describes an inhomogeneous broadening mechanism that is the result of dispersion of the effective stiffness fields in reciprocal k -space associated with a distribution of spin-waves. If we assume that k_{max} is an inverse function of the waveguide width w , then we can show (see Appendix) that the enhancement of the measured linewidth should be a quadratic function of both reciprocal resonance frequency ω_0^{-1} and normalized film thicknesses $\delta_w \doteq \delta/w$, through a Taylor's series expansion of Eq. (1) in the limit of $(\omega_s(k_{\text{max}}) - \omega_0) \ll \Delta\omega_{\text{int}}$. The final result is

$$\beta \approx \alpha + \frac{\pi^2 \omega_M^2}{32 \alpha} \left(\frac{\delta_w}{\omega_0} \right)^2, \quad (2)$$

where $\beta \doteq 2/\tau\omega_M$ is the normalized decay rate, τ is the exponential relaxation time constant associated with the free induction decay of the gyromagnetic precession, α is the LLG damping parameter, and $\omega_M \doteq \gamma\mu_0 M_S$.

We extracted the intrinsic line-width of our samples using fits described below [see Eq. (3)] that extend to about 4 GHz resulting in the following fitted values for the equivalent LLG damping for our films: $\alpha=0.0076$ ($\delta=25$ nm), $\alpha=0.0081$ ($\delta=46$ nm), $\alpha=0.0094$ ($\delta=68$ nm), and $\alpha=0.011$ ($\delta=93$ nm). Figure 1 shows the normalized decay rate β as a function of resonance frequency for five different values of δ_w . The LLG contribution to the damping α was subtracted from each data set in the figure to facilitate easy comparison. The data included in Fig. 1 were obtained using all three CPWs and the 25, 68, and 93 nm films. The particular values of the CPW center conductor width and film thickness were chosen to minimize the overlap in the data for clarity of presentation. The overall trend in the data is a larger enhancement of the decay rate at low frequencies as the value of δ_w increases. While this trend is qualitatively consistent with the predictions of Eq. (1), the quantitative predictions for the frequency dependence of the damping are much smaller than what is measured.

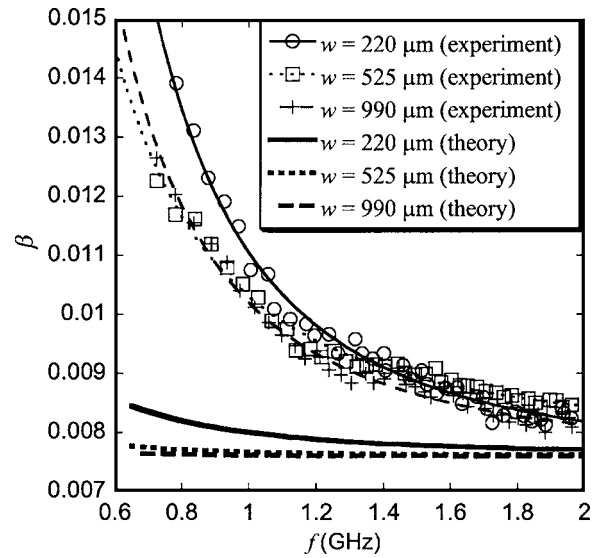


FIG. 2. The normalized decay rate data are shown for the $\delta=25$ nm film. The fits to the data using Eq. (3) are shown as lines through the data. The predicted behavior using Eq. (1) is shown for $\delta=25$ nm film with thicker lines, which do not go through the data at low frequencies.

The data in Fig. 2 shows the normalized decay rate as a function of resonance frequency for the 25-nm thick film on three different waveguide widths. The data were fit using a power law of the form

$$\beta = \alpha + \left(\frac{\nu}{f} \right)^2, \quad (3)$$

where ν is a phenomenological frequency scaling fitting parameter for the power law fit. Using Eq. (3) we are able to quantitatively compare our data to the predictions of Eq. (1). In the limit of small δ_w , one expects an exponent of 2 for contributions to the decay rate that result from the excitation of magnetostatic spin-waves, with $\nu = (\omega_M \delta_w / 8\sqrt{2}\alpha)^5$. The fits of the data to Eq. (3) are shown in Fig. 2, and are in excellent agreement with the data. The lines below the data are the predicted total damping as calculated using Eq. (1). The predicted damping does not agree with the data, as can be clearly seen in Fig. 2.

Figure 3 shows ν taken from our fits of the data to Eq. (3). The data in Fig. 3 are fit well with a line of slope 90 ± 4 GHz and an intercept of 0.0501 ± 0.0005 GHz. The dotted line in Fig. 3 is the prediction based upon Eq. (1) in the limit of small δ_w . Note that the predicted slope of 181 GHz is twice the measured slope. Equation (1) does not predict a non-zero intercept for ν as a function of δ_w . Thus, while we observe low frequency damping behavior suggestive of the spin-wave mechanism proposed in Ref. 5, such a mechanism is not sufficient to account for all of the low-frequency enhancement of the damping that was measured. The data in Ref. 5, Fig. 17 were also fitted to Eq. (3), for comparison with our results. We find that these data do not perfectly follow the predictions of Eq. (1) either.

The distinction between the theoretical predictions of Eq. (1) and our measured data is clearly seen when we consider the normalized decay rate at specific frequencies, independent of any particular equation used to fit the data. Table I presents the normalized decay rate at 1 and 2 GHz, both as experimentally measured and as predicted by Eq. (1). At

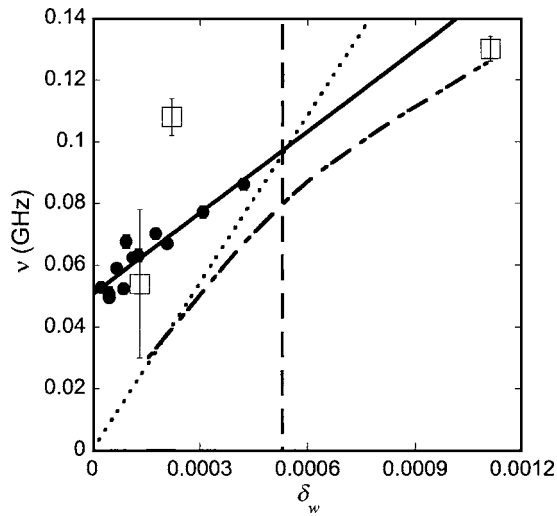


FIG. 3. The value of the power-law scaling frequency ν is plotted as a function of the normalized film thickness δ_w . A linear regression fit to our data is shown as a solid line, with a resultant slope of 90 ± 4 GHz and an intercept of 0.0501 ± 0.0005 GHz. The linear approximation for Eq. (1) for $\alpha = 0.008$ in the limit of small δ_w , is shown as the dotted line. Also shown as the dot-dash line are calculated values for ν based upon numerical fitting of Eq. (1) with Eq. (3) assuming an $\alpha = 0.006$. The data extracted from Ref. 5 and fit to our Eq. (3) are shown as open squares with two σ error bars. The range of validity for the linear approximation is shown to the left of the vertical dash line.

2 GHz, the predicted decay rate is within 2σ of the measured value. However, at 1 GHz, the measured values of decay rate do *not* agree with those predicted by Eq. (1). Thus, it should be emphasized that the deviation of the data from the theoretical prediction of Eq. (1) is clearly observable only for experiments where the gyromagnetic frequencies are less than 2 GHz.

As can be seen in both Fig. 3 and Table I, there is a marked offset between the damping that is measured at low frequencies and what is predicted by Eq. (1). While the low-frequency decay rate depends strongly on δ_w , we find that there is a significant additional component that is independent of δ_w , *but which still scales inversely with ω_0^2* . However, such an enhancement of the measured damping was not observed in Ref. 5, which employed a $45\text{-}\mu\text{m}$ coplanar excitation source and a vector network analyzer to perform the measurements.⁵ Since both the measurements presented here and those of Ref. 5 rely upon a similar waveguide geometry to excite and detect magnetization dynamics, it is not likely that the details of the experimental geometry are responsible for the observed difference between our results and those of Council *et al.* We speculate that there may be a difference between the films used by Council *et al.* and ourselves. For example, both the sign and magnitude of the magnetostriction for permalloy films depend sensitively upon the exact stoichiometry, even if the films in question are nominally $\text{Ni}_{81}\text{Fe}_{19}$. The exact value for the magnetostriction could have significant impact upon the measured dynamical properties. The magnetostriction for the films used in this study was $\lambda_s = 6.7 \times 10^{-7}$, suggesting that our films are very close to the standard permalloy zero-magnetostriction stoichiometry of $\text{Ni}_{81}\text{Fe}_{19}$. Further investigation into this subject is warranted.

TABLE I. Damping values at $f=1$ and 2 GHz are presented for the five data sets seen in Fig. 1. Measurements and the predictions from Eq. (1) are shown and have been normalized by subtracting the LLG damping component.

δ_w	$\beta - \alpha$	$\beta - \alpha$	$\beta - \alpha$	$\beta - \alpha$
	experimental	theoretical	experimental	theoretical
	@ 1 GHz	@ 1 GHz	@ 2 GHz	@ 2 GHz
0.000025	0.0026 ± 0.0004	0.0000	0.0008 ± 0.0004	0.0000
0.000130	0.0036 ± 0.0006	0.0004	0.0003 ± 0.0004	0.0001
0.000177	0.0039 ± 0.0006	0.0007	0.0002 ± 0.0004	0.0002
0.000309	0.0058 ± 0.0007	0.0020	0.0007 ± 0.0003	0.0006
0.000423	0.0079 ± 0.0010	0.0032	0.0006 ± 0.0003	0.0010

In conclusion, while the dependence upon δ_w is suggestive of the predictions of conventional magnetostatic mode wave theory,⁵ there appears to be an additional contribution to the low-frequency decay rate. This additional contribution to the decay rate is independent of the relevant experimental geometrical factors of waveguide width and film thickness. The geometry-independent enhancement in the damping at low frequencies is significant at 1 GHz, exhibiting an increase of as much as a 60% in damping compared to that at 2 GHz.

Appendix. As shown in Ref. 5, the resonance frequency for the case of excitation by a waveguide of finite width w is given by

$$\omega_s(k_{\text{max}}) \approx \omega_0 + \frac{\omega_M^2 k_{\text{max}} \delta}{4\omega_0}. \quad (\text{A1})$$

Substituting into Eq. (1) and using the approximation $(\omega_s(k_{\text{max}}) - \omega_0) \ll \Delta\omega_{\text{int}}$:

$$\Delta\omega(k_{\text{max}}) \approx \Delta\omega_{\text{int}} + \frac{\pi^2 \omega_M^4}{32 \Delta\omega_{\text{int}}} \left(\frac{\delta_w}{\omega_0} \right)^2. \quad (\text{A2})$$

Converting to the normalized decay rate β :

$$\beta \approx \alpha + \frac{\pi^2 \omega_M^2}{32 \alpha} \left(\frac{\delta_w}{\omega_0} \right)^2. \quad (\text{A3})$$

The range of validity for this approximation is

$$\left(\frac{4 \alpha \omega_0}{\pi \omega_M} \right)^2 \gg \delta_w^2. \quad (\text{A4})$$

¹T. J. Silva, C. S. Lee, T. M. Crawford, and C. T. Rogers, J. Appl. Phys. **85**, 7849 (1999).

²C. Alexander, J. Rantschler, T. J. Silva, and P. Kabos, J. Appl. Phys. **87**, 6633 (2000).

³A. B. Kos, T. J. Silva, and P. Kabos, Rev. Sci. Instrum. **73**, 3563 (2002).

⁴G. Council, J. V. Kim, K. Shigeto, Y. Otani, T. Devolder, P. Crozat, H. Hurdequint, and C. Chappert, J. Magn. Magn. Mater. **272–276** (Pt. 1), 290 (2004).

⁵G. Council, K. Joo-Von, T. Devolder, C. Chappert, K. Shigeto, and Y. Otani, J. Appl. Phys. **95**, 5646 (2004).

⁶Y. Ding, T. J. Klemmer, and T. M. Crawford, J. Appl. Phys. **96**, 2969 (2004).

⁷M. L. Schneider, A. B. Kos, and T. J. Silva, Appl. Phys. Lett. **85**, 254 (2004).

⁸J. P. Nibarger, R. Lopusnik, and T. J. Silva, Appl. Phys. Lett. **82**, 2112 (2003).